Charge Resonance Effects on Electronic Absorption Line Shapes: Application to the Heterodimer Absorption of Bacterial Photosynthetic Reaction Centers

Huilin Zhou and Steven G. Boxer*

Department of Chemistry, Stanford University, Stanford, California 94305-5080

Received: March 5, 1997; In Final Form: May 22, 1997[⊗]

The electronic absorption spectrum of the homodimeric special pair in bacterial photosynthetic reaction centers is greatly modified when one of the bacteriochlorophylls is replaced by a bacteriopheophytin to form a heterodimer. The absorption exhibits further unusual changes when hydrogen bonds from the protein to conjugated carbonyl groups are added or removed. In order to explain these absorption features, we postulate a charge resonance interaction between the lowest energy exciton state of the special pair and an intradimer charge transfer state. A general theory is developed that is closely related to the formalism of Fano's treatment for atomic absorption line shapes associated with autoionization (Fano, U. *Phys. Rev* **1961** *124,* 1866). Three different charge resonance limits are discussed, which depend on the relative magnitudes of the electronic coupling between the exciton state and charge transfer state and the vibronic bandwidth of the charge transfer state. In the intermediate charge resonance limit, two broad bands are predicted, and this corresponds closely to the unusual absorption line shape observed for the heterodimer. Furthermore, the systematic variations in the absorption line shapes for four different heterodimer/hydrogen bond mutants can be satisfactorily explained by shifting the relative energies of the exciton and charge transfer states. This leads to the conclusion that the $BChl^+BPhe^-$ intraheterodimer charge transfer state is primarily responsible for the charge resonance interaction, providing information on the absolute energy of this functionally-relevant state and the electronic coupling. This treatment is generally applicable to absorption line shapes in related systems and can be used to provide a unified treatment of the absorption spectra of a large variety of available perturbed homo- and heterodimers.

Introduction

The initial electron transfer reaction in bacterial photosynthesis occurs from the singlet excited state of a strongly interacting pair of bacteriochlorophylls (BChls) called the special pair or P.[1,2] Because dimeric electron donors appear to be a common feature of many photosynthetic reaction centers (RCs), it has long been suspected that some feature of the excited state electronic structure of this dimer is important for efficient charge separation. In particular, there has been much discussion of the role of charge transfer (CT) states of the dimer.[3−8] In the simplest one-electron picture, degenerate intradimer charge transfer states, in which an electron is transferred from one chromophore to another within the dimer, are expected to be close in energy to locally-excited and exciton states of the dimer. In wild-type bacterial RCs, there is good evidence that the two monomeric bacteriochlorophylls (BChls) comprising the dimer, denoted $BChl_L$ and $BChl_M$, are not equivalent due to interactions with the ordered protein environment, which creates a large and asymmetric local electric field,[9] and due to specific hydrogen bonds from the protein to conjugated carbonyl groups of the monomers comprising P.[10−12] In this case the intradimer charge transfer states $BChl_L^+BChl_M^-$ and $BChl_L^-BChl_M^+$ are not degenerate; however, their energy ordering and difference are not obvious, and one of them may preferentially mix with exciton states of the dimer depending on their absolute energies.

The heterodimer special pair denoted D, which forms when the axial histidine M202 coordinated to $BChl_M$ is changed to leucine, is an extreme case of an unsymmetric perturbation.[13,14] This mutation leads to the loss of Mg and conversion of $BChl_M$ to a bacteriopheophytin (BPhe) as shown schematically in Figure 1. Because BPhe is substantially easier to reduce electrochemically *in vitro*,[15] it is likely that the $BChl^+BPhe^-$ state of the heterodimer is lower in energy than the $BChl^-BPhe^+$ state; however, the energy difference in the RCs and the relevant absolute energies of these states relative to the exciton states of D are not known. The absorption spectrum of the heterodimer special pair is strikingly different from the wild-type (WT)

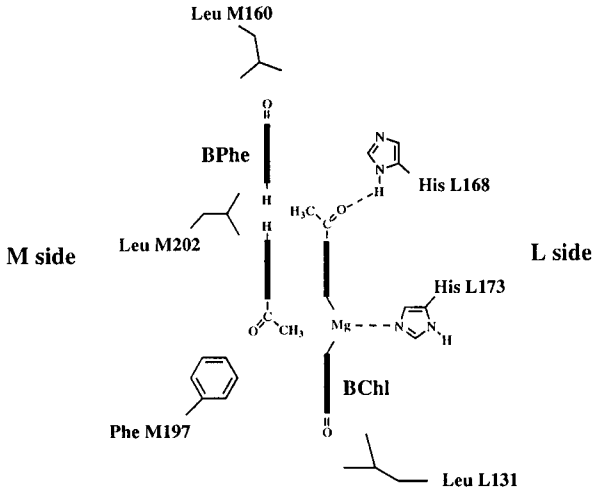

Figure 1. Schematic diagram of the heterodimer special pair in *Rb. sphaeroides* (M)H202L mutant RCs including key amino acid residues in the vicinity of the dimer. Replacement of histidine M202 in wild-type by leucine leads to the formation of the heterodimer where Mg is lost from the bacteriochlorophyll on the M-side to form a bacteriopheophytin. Histidine L168 is hydrogen bonded to the conjugated acetyl carbonyl group of the L-side BChl in the heterodimer mutant. Conversion of phenylalanine M197 to histidine creates a new hydrogen bond to the M side chromophore;[10−12,37] likewise conversion of leucine M160 and/or L131 to histidine creates new hydrogen bonds to the conjugated C-9 keto carbonyl groups of the macrocycles.[10−12,37]

[⊗] Abstract published in *Advance ACS Abstracts,* July 1, 1997.

S1089-5647(97)00828-6 CCC: $14.00

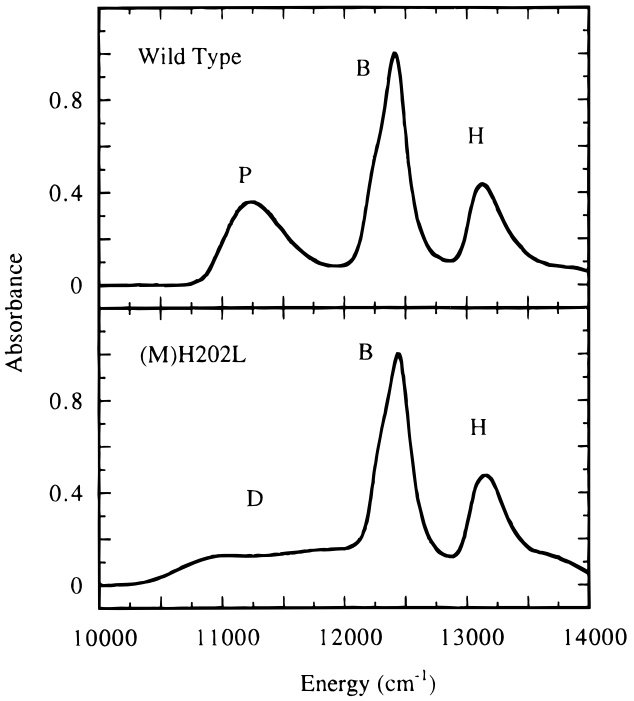

Figure 2. Absorption spectra of *Rb. sphaeroides* wild-type (upper panel) and heterodimer (M)H202L mutant (lower panel) RCs at 77 K. For WT the special pair absorption is labeled P, while for the heterodimer the two broad absorption bands are labeled D. The accessory monomeric BChl and BPhe absorption bands are labeled B and H, respectively. The spectra are normalized to unit absorbance at the maximum of the B band.

homodimer as shown in Figure 2. At room temperature, the heterodimer absorption is featureless, but at low temperature it is seen to consist of two poorly resolved, broad bands of roughly equal area centered at 850 and 920 nm.[4] The total area under these two bands in heterodimer RCs is comparable to that of the P band in WT RCs using the area under the B (two monomeric BChls) or H bands (BPhes) in both types of RCs as internal standards. The lowest electronic absorption of P is unusually broad at 77 K ($\sim$500 cm^{-1}) compared with a monomeric BChl ($\sim$100$-$200 cm^{-1}). Extensive hole burning studies have revealed that the P band is mostly homogeneously broadened at cryogenic temperature,[16$-$18] and a large electron$-$phonon coupling has been proposed to account for this.[16$-$19] The origin of the large electron$-$phonon coupling has not been established, but it is not unexpected when excitation of the chromophore involves a substantial displacement of charge, e.g. for a transition with substantial charge transfer character. Consistent with this, it has been shown by Stark spectroscopy that the difference in permanent dipole moment between the ground and excited state, $\Delta\mu$, for P is substantially larger than for a monomeric BChl,[5,9] and it is much larger still for both transitions of the heterodimer special pair.[4] Two additional observations are important for the heterodimer. First, selective excitation of the feature at 920 nm at cryogenic temperatures leads to bleaching of both this feature and that at 850 nm; thus, these transitions share a common ground state.[20] Likewise, excitation at 532 nm leads to a bleaching of both the 920 and 850 absorption bands when D^+ is formed in proporption to their ground state absorption. Thus, both transitions are associated with the heterodimer, and these are not localized transitions due to the monomeric bacteriochlorophyll and bacteriopheophytin comprising the heterodimer (i.e. we treat the heterodimer as a supermolecule). Second, selective excitation of the higher energy feature at 850 nm leads to an instrument-response-limited rise in the fluorescence at 970 nm associated with the lower energy transition with a polarization close to 0.4.[21] Thus the transition moments of the two features are approximately parallel, and the two bands are not the lower and upper exciton bands of D whose transition moments should be approximately perpendicular.

No conventional electron$-$phonon coupling model can explain the presence of two relatively broad and equally intense absorption bands for D. Lathrop and Friesner have presented a theoretical analysis of the heterodimer absorption spectrum.[7,8] Their treatment considered only the lower energy band (920 nm band), and the relationship between their model and ours will be discussed further below. In the course of studies of the Stark effect spectra of RCs containing heterodimers in which peripheral hydrogen bonds to histidine residues have been added or removed by preparing mutants at residues L168, M197, M160, and L131 (see Figure 1), we noticed that there were interesting variations in the line shapes and positions of the two features. In the following we develop a theoretical model which can account for these variations and which can be further used to obtain information on the energies of internal charge transfer states of the special pair relative to exciton states which may be relevant for understanding the charge transfer process. In subsequent papers this model will be used to provide a unified description of the wild-type special pair and a variety of homodimer/hydrogen bond mutant absorption spectra, the Stark spectra of these mutants, and novel features observed in the higher order Stark spectra of RCs associated with other functionally-significant charge transfer states.

Theory

We consider three states: the ground state ψ_0, the pure molecular exciton state ψ_1, and one intradimer charge transfer state ψ_{CT} of the special pair (we do not consider coupling to other charge transfer states involving the other chromophores as these are expected to be much weaker than coupling to the intradimer charge transfer state[6]). The Born$-$Oppenheimer approximation is assumed for all three states. The optical transition from the ground state to the exciton state with energy ω_0 on the order of 10 000 cm^{-1} is strongly allowed. In the absence of charge displacement, both the ground state ψ_0 and pure molecular exciton state ψ_1 are assumed to have the same nuclear wavefunctions, and the transition from ψ_0 to ψ_1 is vibronically discrete. On the other hand, the intradimer charge transfer state should have a very different nuclear wavefunction from ψ_0 and ψ_1 as a result of large electron$-$phonon coupling. ψ_{CT} is assumed to lie energetically in reasonable proximity to ψ_1; thus, we will only consider the charge resonance interaction between ψ_{CT} and ψ_1 and not that between ψ_{CT} and ψ_0. At infinite separation between the electron donor and acceptor, a direct intermolecular (intradimer) CT transition has a vanishing transition probability. As the intermolecular distance between the donor and acceptor decreases, transition to the CT state gains more transition probability as the charge resonance interaction between ψ_{CT} and ψ_1 increases. It is assumed that the final state can always be approximated as a linear combination of both the ψ_1 and ψ_{CT} states, and the observed absorption line shape is a result of transition from the ground to this final state.

Because ψ_{CT} is vibronically broad with respect to ψ_1, the charge resonance interaction between the ψ_1 and ψ_{CT} states can be viewed as a resonance interaction between a vibronically discrete state and a vibronically broad state. Quantum interference effects between a discrete state and a broad molecular dissociation state was discussed by O. K. Rice for the predissociation region of molecular spectra. He showed that the absorption line shape is both broadened and shifted by such an

interference effect.[22] Fano considered a similar quantum interference effect for atomic absorption line shapes in the case of the atomic autoionization.[23] It has been shown that the formalism of Fano theory also applies when the continuum state is a vibronic continuum.[24] As formulated, the present problem is analogous to the Fano resonance, the difference being that the ionization continuum in Fano's treatment is replaced by a vibronic continuum.

The pure electronic coupling term between the exciton state ψ_1 and ψ_{CT} is defined as V_0. The vibrational overlap function $G_2(\omega)$ between ψ_1 and ψ_{CT} must be included in the charge resonance interaction. The diagonalization between the ψ_1 and ψ_{CT} states is straightforward and follows the Fano treatment,[23] yielding a superposition between ψ_1 and ψ_{CT}. The absorption line shape from the ground state to this final state is given as

$$\epsilon_2(\omega) = \frac{|V_0|^2 G_2(\omega)}{[\omega - \omega_0 - |V_0|^2 G_1(\omega)]^2 + \pi^2 |V_0|^4 G_2(\omega)^2} \quad (1)$$

where $\epsilon_2(\omega)$ is the imaginary part of the dielectric function, i.e., the absorption coefficient. It is understood that the amplitude of $\epsilon_2(\omega)$ needs to be scaled by a constant for comparison with experimental absorption spectra because the transition probability from ψ_0 to ψ_1 is not included. $|V_0|^2$ is the absolute square of the pure electronic coupling term between ψ_1 and ψ_{CT}. $|V_0|^2 G_2(\omega)$ thus has the dimension of energy because $G_2(\omega)$ is normalized "per unit energy" as shown below. $|V_0|^2 G_2(\omega)$ basically describes the electron transfer rate in conventional electron transfer theories, as will become evident below.[25−27] $G_1(\omega)$ is the Hilbert transform of $G_2(\omega)$

$$G_1(\omega) = P\int_{-\infty}^{\infty} \frac{G_2(\omega')\, d\omega'}{\omega - \omega'} \quad (2)$$

where P denotes the Cauchy principal value of the integral.

The vibrational overlap function $G_2(\omega)$ is of crucial importance in many electron transfer theories.[25−27] In many studies of linear electron−phonon coupling, it is expected to have a nearly symmetric and broad Gaussian line shape.[28,29] Here we assume it to have a Gaussian line shape for simplicity, recognizing that the actual line shape may deviate somewhat and this will affect a quantitative analysis

$$G_2(\omega) = \frac{2}{\Delta_{CT}}\sqrt{\frac{\ln 2}{\pi}} \exp\left[-4\left(\frac{\omega - \omega_{CT}}{\Delta_{CT}}\right)^2 \ln 2\right] \quad (3)$$

where Δ_{CT} is the full width at half-maximum (fwhm) of $G_2(\omega)$, whose maximum value is at ω_{CT}. It is evident from eq 3 that $G_2(\omega)$ has the dimension of "per unit energy". $G_1(\omega)$ can be calculated numerically from eq 2. It is convenient to use a reduced energy variable ξ, defined as $\xi = (\omega - \omega_0)/\Delta_{CT}$. If $\omega_{CT} = \omega_0$, $G_2(\xi)$ and $G_1(\xi)$ as functions of this reduced energy variable ξ are shown in Figure 3. In the following we examine the absorption line shape in eq 1 as a function of the coupling strength V_0, the bandwidth Δ_{CT} of $G_2(\omega)$, and the location of ψ_1 within the vibronic continuum of ψ_{CT}. It is further useful to parameterize the problem in terms of the relative coupling strength $R = V_0/\Delta_{CT}$ and the relative energy shift $\delta = (\omega_0 - \omega_{CT})/\Delta_{CT}$ which characterizes the relative location of the ψ_1 state within the vibronic continuum of the ψ_{CT} state. V_0 is usually a complex quantity; here it is understood as a real quantity for simplicity.

The problem naturally divides into the following three cases.

Case I. The vibronically discrete state ψ_1 is located at ω_{CT}, i.e. at the maximum of $G_2(\omega)$, so $\delta = 0$. This case corresponds to an activationless electron transfer process from the ψ_1 state because the potential surface of ψ_{CT} intersects the bottom of that of ψ_1 state. The bandwidth Δ_{CT} of $G_2(\omega)$ is directly related to the reorganization energy in Marcus theory.[25,30] The upper panel of Figure 4 shows the effect of varying the relative coupling strength R and leads to a further classification of calculated line shapes.

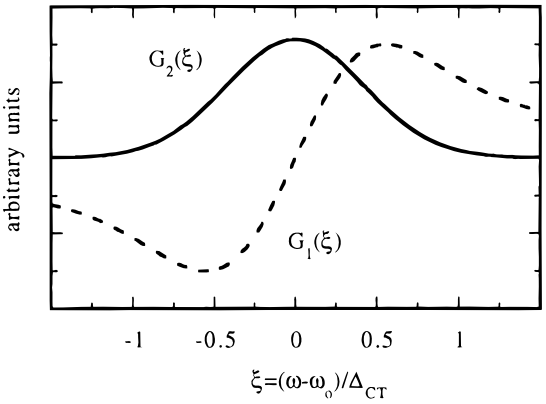

Figure 3. Dependence of the vibrational overlap function $G_2(\xi)$ (—) and its Hilbert transform $G_1(\xi)$ (- - -) on the reduced energy variable $\xi = (\omega - \omega_0)/\Delta_{CT}$ ($\omega_{CT} = \omega_0$ in eq 3). They have similar amplitudes.

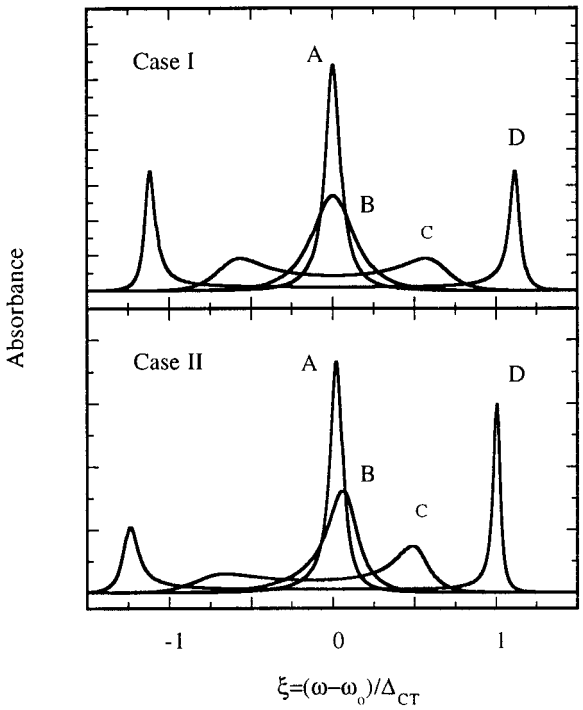

Figure 4. Calculated absorption line shapes derived from eq 1 as a function of the relative coupling strength $R = V_0/\Delta_{CT} = 0.13$ (curves A), 0.2 (curves B), 0.5 (curves C), and 1.0 (curves D) for case I (upper panel) where the vibronically discrete state ψ_1 is located at ω_{CT}, the maximum of $G_2(\omega)$, and case II where ψ_{CT} is shifted to the lower energy side of ω_0 ($\delta = +0.2$, see text). For case III, where ψ_{CT} is shifted to the higher energy side of ω_0 (δ is negative), the absorption line shapes (not shown) are reversed about $\xi = 0$ compared with case II.

Weak Charge Resonance Limit. If the relative coupling strength R is small, for example $R = 0.13$ (curve A in the upper panel of Figure 4), the absorption line shape is approximately a single Lorentzian. Because the electronic coupling V_0 is much smaller than the bandwidth Δ_{CT} of $G_2(\omega)$ and the ψ_1 state is located at the peak of $G_2(\omega)$, $G_1(\omega)$ nearly vanishes while $G_2(\omega)$ is almost constant, *cf.* Figure 3. The absorption spectrum is approximately Lorentzian as can be seen clearly from eq 1 (because of the nonzero value of $G_1(\omega)$ at $\omega \neq \omega_{CT}$, the

absorption line shape in eq 1 is never strictly Lorentzian). The line width of this quasi-Lorentzian absorption reflects the lifetime broadening of the discrete state ψ_1 "decaying" into the state ψ_{CT}, equivalent to an excited state electron transfer process with electron transfer rate $\pi|V_0|^2G_2(\omega)$. As the relative coupling strength R increases to 0.2 (curve B in Figure 4), the line shape remains approximately Lorentzian; however, its absorption peak value decreases and its line width is homogeneously broadened, i.e., the electron transfer process speeds up.

Intermediate Charge Resonance Limit. As the relative coupling strength R further increases to 0.5, where the coupling strength V_0 is equal to the half-width $\Delta_{CT}/2$ of $G_2(\omega)$, the single Lorentzian-like band in the weak charge resonance limit is replaced by two broad bands (curve C, upper panel in Figure 4). These two bands are broad and symmetric with respect to $\xi = 0$. In this intermediate charge resonance limit, the Born−Oppenheimer approximation will no longer be valid for the final state, and the electron transfer dynamics between the donor and acceptor are expected to depend strongly on nuclear geometry changes. In this one-electron resonance picture, only the electron from the donor is being considered. The broad line width suggests that this electron is neither localized on the donor nor is it completely delocalized on the donor−acceptor complex, which would result in a stable final state as shown below.

Strong Charge Resonance Limit. As the relative coupling strength R increases further to 1.0 where V_0 is equal to the full width Δ_{CT} of $G_2(\omega)$, the two-band splitting line shape becomes much more evident and the line width of each begins to decrease (curve D, upper panel in Figure 4). For even larger R, these two narrow bands are sharper and further apart (not shown), which is exactly what one expects from a simple molecular orbital picture of two interacting degenerate states. The electron from the donor is expected to be highly delocalized over both states ψ_1 and ψ_{CT}, and the narrow line width of the two bands reflects the fact that the electron-delocalized state is stable. The lower energy band can be viewed as a transition to a bonding state, while the higher energy band is a transition to an antibonding state.

Case II. The vibronically discrete state ψ_1 is located at the high-energy side of ω_{CT}, the maximum of $G_2(\omega)$, i.e., ψ_{CT} is shifted to lower energy compared to case I. The relative energy shift term δ is positive for case II; for the purpose of discussion, δ is chosen as $+0.2$.

Weak Charge Resonance Limit. For $R = 0.13$ an asymmetric quasi-Lorentzian line shape is predicted (curve A, lower panel in Figure 4). Close examination shows that its higher energy side is sharper and the peak position is shifted to higher energy compared to curve A for case I in the upper panel. As R increases to 0.2, the asymmetric quasi-Lorentzian line shape broadens and the asymmetry becomes more pronounced (compare curve B in the upper and lower panel of Figure 4). Furthermore, the peak shifts to higher energy in case II compared to case I. The charge resonance interaction between ψ_1 and ψ_{CT} thus causes a resonance bandshift in addition to band broadening. Such a resonance energy shift (from the term $|V_0|^2G_1(\omega)$ in eq 1) is directly related to the bandwidth $|V_0|^2G_2(\omega)$ of the transition to the final state through the Hilbert transformation. This phenomenon was also discussed by Rice in molecular predissociation spectra and Fano in autoionization processes.[22,23] In general, the symmetry of $G_2(\omega)$ with respect to $\omega = \omega_0$ is the key factor in determining the symmetry of the absorption line shape to the final state, which is characterized here by the relative shift term δ.

Intermediate Charge Resonance Limit. For $R = 0.5$, two broad bands are predicted (curve C in the lower panel of Figure 4). In contrast to curve C in the upper panel, these two bands are not identical, and their asymmetry is determined solely by the relative shift term δ. The line width of the higher energy band is relatively smaller than that of the lower energy band, which also has less absorbance because this band has a larger contribution from the CT state to which transition from the ground state is forbidden. Conversely, the narrower higher energy band has more contribution from the ψ_1 state, to which transition from ground state is allowed. Because the most significant mixing between ψ_1 and ψ_{CT} occurs at the same nuclear geometry as the ground state and the potential energy of the ψ_{CT} state is lower than ψ_1, the lower energy band should have more contribution from ψ_{CT} from a simple molecular orbital interaction argument. Finally, the broader band at lower energy itself has an asymmetric line shape, with the lower energy side sharper than the higher energy side. The opposite line shape asymmetry is found for the higher energy band: its higher energy side is sharper than its lower energy side.

Strong Charge Resonance Limit. For $R = 1.0$, two *narrow* bands are again observed (curve D, lower panel in Figure 4); however the peaks are not equivalent, as the lower energy band is relatively broader and less intense with more CT state character, while the higher energy band is sharper and more intense. Such line shape asymmetry is only related to the relative shift term δ. Again, the narrow line shape reflects the fact that the electron-delocalized states are stable.

Case III. The vibronically discrete state ψ_1 is located at the low-energy side of ω_{CT}, the maximum of $G_2(\omega)$, i.e., ψ_{CT} shifts to higher energy compared to case I, and δ is negative. In this case we expect the opposite behavior to those illustrated in the lower panel of Figure 4 by simply reversing the scale of the abscissa about $\xi = 0$ for the same values of R (not shown).

In summary, there is a smooth transition of the absorption line shapes among the three charge resonance limits, which depends only on the relative coupling strength R. The overall *line width* of the experimental absorption spectrum depends on both the relative coupling strength and the bandwidth Δ_{CT} of $G_2(\omega)$; however, its *line shape* does not depend on Δ_{CT}. Note that the integrated oscillator strength is conserved in all cases because the diagonalization of ψ_1 and ψ_{CT} is a unitary transformation. The relative coupling strength R is the defining parameter for the three charge resonance limits, while the relative shift δ determines the degree of equivalence of the oscillator strength and line shape of the two absorption bands. In the weak charge resonance limit, the absorption line shape resembles a Lorentzian whose line width is directly related to the excited state electron transfer lifetime. The resonance energy shift depends on both the *relative* coupling strength between these two states and the *relative* shift δ between ω_0 and ω_{CT}. In the intermediate charge resonance limit, two broad bands are predicted, and one expects the electron transfer dynamics to be strongly correlated with the nuclear motion. In the strong charge resonance limit, the electron from the donor is delocalized between the donor and acceptor and two narrow bands are expected with the spectral splitting being approximately $2V_0$ as one expects from a simple molecular orbital picture.

In the weak charge resonance limit where the dynamics of photoinduced electron transfer reactions are often studied, the homogeneous line width of an absorption band due to electron transfer dynamics is likely to be overwhelmed by inhomogeneous broadening mechanisms in the condensed phase, and it is necessary to use hole-burning spectroscopy to get dynamical information from the absorption spectrum. Stark spectroscopy is also useful because the energy of a coupled CT state is altered by the applied electric field, and as shown above, such an energy

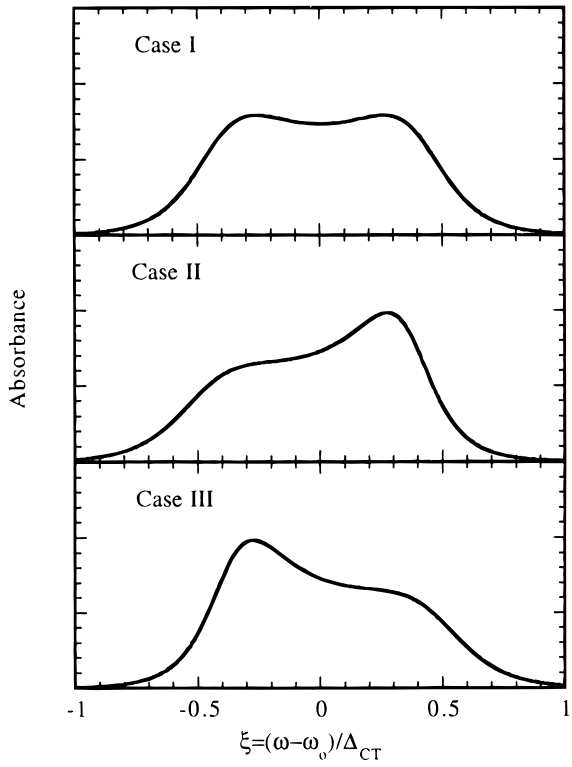

Figure 5. Calculated absorption line shapes in the intermediate charge resonance coupling limit as the relative shift term δ is varied. For case I, $\delta = 0.0$ and ψ_1 is located at ω_{CT}; for case II, $\delta = +0.1$ and ω_{CT} is shifted to the lower energy side of ψ_1; for case III, $\delta = -0.1$ and ω_{CT} is shifted to the higher energy side of ψ_1.

shift has a marked effect on the absorption line shape to the final state.[31] The homogeneous line width in the intermediate charge resonance limit could be very large and may become the dominant broadening mechanism. An electronic coupling strength on the order of hundreds of wavenumbers has been demonstrated in a number of cases.[32]

As shown below, the intermediate charge transfer limit appears to apply to the heterodimer case, so we consider this further. Figure 5 illustrates the absorption line shapes when the relative shift is varied with R being fixed at 0.35. Figure 5A shows the absorption spectrum for $\delta = 0$; two broad equivalent bands are expected. As $G_2(\omega)$ shifts to lower energy, i.e. the relative shift δ is positive, the lower energy band becomes broader with less absorbance, while the higher energy band becomes sharper with more absorbance (Figure 5B where $\delta = +0.1$). The opposite behavior is observed if δ is negative ($\delta = -0.1$) as shown in Figure 5C. Information about the relative coupling strength can be deduced from the extent of band splitting, and the relative shift can be inferred from their line shapes. For example, the line shapes of the lower energy bands in Figure 5 also depend on the relative shift term, and the relative shift can also be inferred from their relative peak absorption.

Methods

The heterodimer and heterodimer/hydrogen bond double mutants[12] were grown semianaerobically. Reaction centers were isolated using standard methods.[33] RCs in 0.1% LDAO, 10 mM Tris buffer (pH 8.0) were mixed with an equal volume of glycerol, and absorption spectra were obtained at 77 K.

As seen in Figure 2, the higher energy feature of the two broad heterodimer absorption bands overlaps somewhat with the relatively sharp absorption associated with the monomeric BChls labeled B and centered around 800 nm. As shown below, the D absorption bands shift and have a different separation and variable amplitudes and line shapes in different hydrogen bond/heterodimer mutants, and this changes the spectral overlap between the upper feature of D and the B band. In addition the B band position shifts slightly in different mutants (the B band consists of overlapping absorptions due to both B_L and B_M, and small shifts in their absorption maxima and widths change the overall shape of the 800 nm feature), and it is difficult to obtain a perfectly flat base line in all samples at 77 K. Because of these uncertainties and because we do not know the line shape of the higher energy heterodimer band *a priori*, we have not attempted to deconvolve the heterodimer special pair and B absorption features. The B band has no overlap with the lower energy D band. In the following, we use the line shape of the lower energy D band (around 910−920 nm) as a *primary* constraint to obtain the relative coupling strength. The relative shift term δ is found by both the relative absorbance of the two heterodimer absorption bands and the line shape of the lower energy band because the relative shift term also affects the lower energy band line shape, cf. Figure 5. It is desirable to obtain some quantitative information about the electronic coupling V_0, the locations of ω_0 and ω_{CT}, and the bandwidth Δ_{CT} of $G_2(\omega)$. As the relative coupling strength and relative shift term are known from the above line shape analysis, we adjust the bandwidth Δ_{CT} of $G_2(\omega)$ and location of ω_0 until the calculated absorption line shape matches the experimental spectrum. The electronic coupling strength V_0 and the location of ω_{CT} can then be readily deduced. This simple data analysis procedure was used to obtain the parameters in Table 1 and the calculated absorption spectra. We stress that given the simplicity of the model and the uncertainties associated with overlap of the higher energy D band and the B band, we only seek to find trends and approximate values of the relevant parameters.

TABLE 1: Parameters Obtained by Comparing the Theoretical Model (Eqs 1 and 3) to the Absorption Spectra (Figures 6 and 8) for Heterodimer/Hydrogen Bond Mutants of *Rb. sphaeroides* Reaction Centers[a]

mutant[b]	ω_0 (cm^{-1})	V_0 (cm^{-1})	Δ_{CT} (cm^{-1})	$\omega_0 - \omega_{CT}$ (cm^{-1})
(M)H202L	11 400	542	1550	46
(M)H202L/(M)F197H	11 285	549	1593	167
(M)H202L/(L)H168F	11 450	536	1625	114
(M)H202L/(M)L160H	10 920	603	1800	225
(M)H202L/(L)L131H	11 600	511	1525	−61

[a] See text for definitions of ω_0, V_0, Δ_{CT} and $\omega_0 - \omega_{CT}$. [b] See Figure 1 for locations of residues.

Analysis and Results

An expanded view of the (M)H202L heterodimer mutant absorption spectrum in the Q_Y region at 77 K is shown in the upper panel of Figure 6. The two absorption features are approximately equal in intensity and line width; a similar result was obtained from the somewhat better resolved spectrum at 1.5 K.[4] By comparison with the model spectra in Figures 4 and 5, these features are qualitatively consistent with placing the heterodimer in the intermediate charge resonance limit with the relative shift term δ close to zero (case I). Because the transition dipoles for these two bands are derived from the same electronic transition from the ground state to the exciton state, they share the same ground state and their transition dipole moments are expected to be parallel, as observed.[21] As described above, we use the lower energy band line shape, which does not overlap with the B band, as a primary constraint to obtain the calculated absorption which is shown in the lower

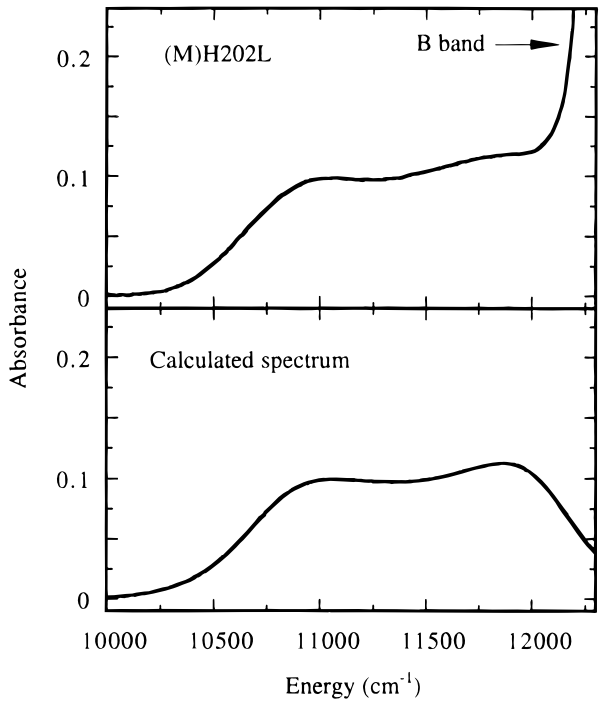

Figure 6. Expanded view of the heterodimer (M)H202L special pair absorption (upper panel) under identical experimental conditions as in Figure 2, and the calculated spectrum obtained using eq 1 and parameters listed in Table 1 (lower panel).

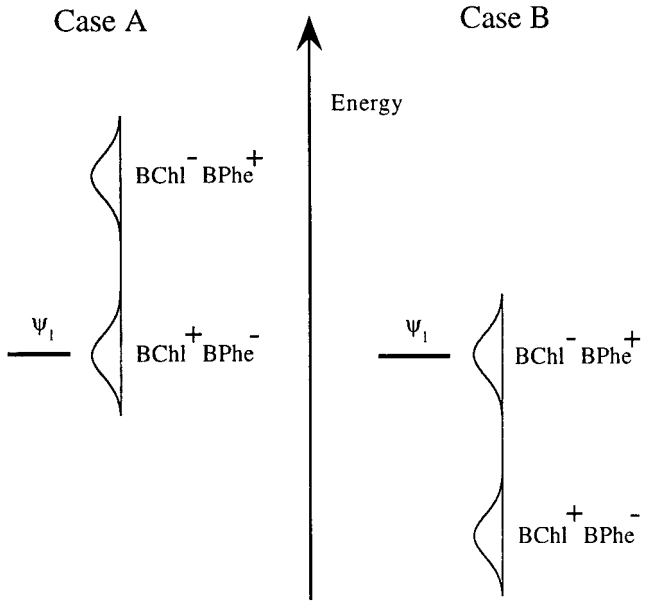

Figure 7. Schematic illustration of two possible arrangements of the absolute energies of the vibronically discrete state ψ_1 and the two broad charge transfer states of the heterodimer. Because BPhe is substantially easier to reduce than BChl *in vitro*, it is assumed that the $BChl^+BPhe^-$ charge transfer state is much lower than the $BChl^-BPhe^+$ charge transfer state. In case A, the dominant charge resonance interaction is between ψ_1 and $BChl^+BPhe^-$; in case B, the dominant charge resonance interaction is between ψ_1 and $BChl^-BPhe^+$. Changes in the arrangements of hydrogen bonds to BChl and BPhe in the heterodimer will further perturb the absolute energies. The results suggest that case A applies.

panel of Figure 6. The coupling strength V_0, line width Δ_{CT} of $G_2(\omega)$, location of the maximum ω_{CT} of $G_2(\omega)$, and location of the exciton state ω_0 are shown in Table 1. As described above, each parameter determines an independent feature of the spectrum, so the calculated spectrum is sensitive to these values.

As discussed in the Introduction, the $BChl^+BPhe^-$ CT state is expected to be substantially lower in energy than the $BChl^-BPhe^+$ CT state because BPhe is much easier to reduce than BChl *in vitro*.[15] Two possible cases for the absolute energies of these states relative to ψ_1 are illustrated in Figure 7. As argued in the following, by systematically analyzing the effects of additional environmental perturbations on the heterodimer absorption caused by adding or deleting hydrogen bonds, it is possible to determine that the heterodimer (M)H202L belongs to case A.

In the (M)H202L/(M)F197H mutant, a hydrogen bond (electron-withdrawing) is added to the acetyl carbonyl group of the BPhe molecule (see Figure 1).[12] This should shift the $BChl^-BPhe^+$ state to higher energy and the $BChl^+BPhe^-$ state to lower energy. It is likely that such energy shifts are considerably smaller than the energy difference between the two CT states; in other words, the effect of hydrogen bond changes on the energy of intradimer CT states is a perturbation on the basic picture. If the absolute energy positioning in case A (Figure 7) applies to the heterodimer (M)H202L, then shifting the $BChl^+BPhe^-$ state energy lower should perturb the experimental absorption spectrum toward a line shape predicted for case II. Conversely, if the absolute energy position in case B (Figure 7) applies, the experimental absorption spectrum should move toward case III. The experimental spectrum is shown in the top panel of Figure 8, and by comparison with the model spectra in Figure 5, the (M)H202L/(M)F197H spectrum shifts toward case II. The calculated absorption spectrum (filled circles) gives excellent agreement for the lower energy band for the parameters listed in Table 1. The spectral overlap between the higher energy band and the B band prevents a more detailed line shape analysis of the higher energy band; however, it is clear that the higher energy band is sharper and has more absorbance while the lower energy band is broader and has less absorbance compared with the (M)H202L heterodimer, the qualitative characteristics expected for case II. Thus we conclude that the $BChl^+BPhe^-$ state is the primary intradimer CT state involved in the charge resonance interaction with state ψ_1 in the (M)H202L/(M)F197H mutant.

A similar analysis was done for the (M)H202L/(L)H168F, (M)H202L/(M)L160H, and (M)H202L/(L)L131H mutants (*cf.* Figure 1), whose absorption spectra are also shown in Figure 8. Again, there is close agreement between the calculated and observed spectra for the lower energy band and qualitative agreement for the higher energy band. In both (M)H202L/(L)H168F and (M)H202L/(M)L160H mutants, either the removal of a hydrogen bond at position (L)168 or an addition of an hydrogen bond at position (M)160, respectively, is expect to lower the intradimer $BChl^+BPhe^-$ state energy; thus, we expect case II to apply as for (M)H202L/(M)F197H, leading to a less intense and broader lower energy band compared with the higher energy band. On the other hand, an additional hydrogen bond on the BChl molecule in the (M)H202L/(L)L131H mutant should increase the energy of $BChl^+BPhe^-$ state; consequently one would expect case III to apply. As seen in the bottom panel of Figure 8, the lower energy band for this mutant is clearly sharper with more absorbance than the higher energy band. Examination of the fit parameters in Table 1 indicates that V_0 and Δ_{CT} are approximately the same for all five mutants, while the primary difference is the position of the CT state relative to the exciton state.

Discussion

We have presented a quantitative theory of various charge resonance limits for excited state electron transfer processes. Related theoretical work on energy transfer was done by

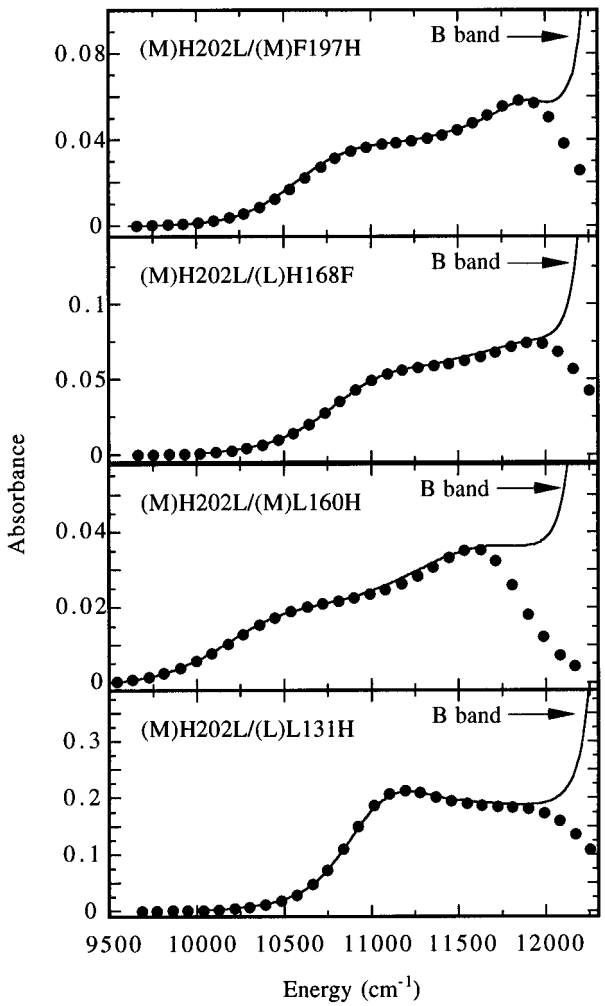

Figure 8. Absorption (—) and best fit to eq 1 (filled circles) for a series of heterodimers in which histidine residues that hydrogen bond to the special pair are added or deleted (*cf.* Figure 1).

Simpson and Peterson[34] who gave a qualitative description of various coupling limits categorized by the relative strength of the resonance energy transfer matrix element and the bandwidth of the Herzberg−Teller vibronic overlap integral. The formal similarity between energy transfer and electron transfer should not be surprising,[27] but the physical nature of the coupling term is very different. The coupling term in the Förster energy transfer mechanism is the transition dipole−transition dipole interaction, while the coupling term for an electron transfer process may be viewed as the interaction of the transition dipole between the neutral and charge-separated states with the electrostatic field from the surrounding nuclei and electrons. We have described three charge resonance limits in which the absorption line shapes are distinctly different. In addition, we have shown that the location of the discrete state within the broad CT state vibronic profile greatly modifies the calculated absorption spectrum, and the symmetry of the absorption line shape and its location are directly correlated to the charge resonance interaction strength.

Comparison of this model with the absorption spectrum of the heterodimer (M)H202L provides an explanation for the presence of two approximately equally intense bands with parallel transition dipole moments and suggests that this is an example of the intermediate charge resonance limit. The observed line shape has not been explained before and comparison with the model indicates that the discrete state is located near the maximum of the broad intradimer $BChl^+BPhe^-$ CT state. When an additional hydrogen bond is added to either the BChl or BPhe half of the heterodimer, one expects a shift in the energy of the $BChl^+BPhe^-$ state with relatively little effect on other properties; consequently, the absorption line shape should change in a well-defined fashion.

The exact form of the vibronic overlap function $G_2(\omega)$ is of primary importance in many electron transfer theories.[25−27] It is expected to be well approximated by a Gaussian line shape and be very broad due to strong electron−phonon coupling for a CT state.[28,29] $G_2(\omega)$ may be somewhat asymmetric;[28,29] this will not affect the line shape comparisons among different heterodimer/hydrogen bond mutants, but the relative shift in each mutant could be modified somewhat. Nonetheless, the primary conclusions still hold that the the lowest energy absorption band of the heterodimer is an example of the intermediate charge resonance limit and that the dominant charge resonance interaction occurs between the intradimer $BChl^+BPhe^-$ state and the discrete state.

The electronic coupling strength V_0 from our analysis of the heterodimer absorption is about the same order of magnitude as that of Parson and Warshel.[6] Lathrop and Friesner also stressed the significance of the interaction between the exciton and intradimer CT states and obtained a coupling strength with similar magnitude.[7,8] Lathrop and Friesner used a detailed set of vibrational modes necessitating a complex simulation; this is replaced in our model with a single Gaussian that leads to the simple analytical expression for the line shape in eq 1. Lathrop and Friesner introduced a "vibronic scaling parameter" A to describe the vibronic coupling to the CT state, and this should correspond to the width of vibrational overlap function we have used. Although it would be desirable to explicitly include coupled modes and their displacements, their values are not known accurately for the low-frequency modes that will dominate. The relative magnitude of the electronic coupling term and the width of the vibrational overlap was not explicitly considered in their work. We conclude that the relative coupling R is the primary factor for categorizing the three limits of the charge resonance interaction, and our analysis shows that the charge resonance interaction in the heterodimer special pair belongs to the intermediate coupling limit, which was not clear before. Finally, the two bands observed for the (M)H202L heterodimer were not discussed by Lathrop and Friesner, but it is evident from the analysis presented here that these two bands and variations in their position, splitting, relative amplitudes, and widths can provide insight into electronic structure of the special pair.

The analysis presented here leads naturally to a parallel treatment of the absorption spectrum of the wild-type homodimer and the effects of perturbations (e.g. by hydrogen bond additions or deletions) on that spectrum. As will be shown elsewhere,[35] large perturbations of the homodimer, e.g. in the (M)L160H mutant, lead to an absorption spectrum which resembles that of the heterodimer in the (M)H202L/(L)L131H mutant. This can be understood because the addition of a hydrogen bond on the L side in (M)H202L/(L)L131H effectively reduces the electron-withdrawing effect on the M side caused by replacing the native M-side BChl with BPhe in the heterodimer. There should be a continuous series from the heterodimer with further electron-withdrawing groups, through the homodimer, to the "reverse" heterodimer [(L)H173L] whose absorption spectrum is very different from the (M)H202L heterodimer discussed here.[36] The theoretical treatment of the homodimer may be more complicated because the splitting between the two charge transfer states is likely to be smaller than for the heterodimer, and it may be necessary to consider

mixing between both and the exciton state(s). Qualitatively one expects offsetting effects if both charge transfer states are included, leading, for example, to smaller values of the excited state dipole moment as is observed. Finally, we note that there are two other "heterodimers" in the reaction center, namely, B_L/H_L and B_M/H_M. The interchomophore distance and geometry in these cases are very different from the heterodimer derived from the special pair, and intuitively one expects a much weaker interaction. As will be shown elsewhere,[31] in the weak charge resonance limit, novel higher order Stark effects are predicted and found from which information can be obtained on excited state electron transfer dynamics from ^1B_L to H_L (or in principle from ^1B_M to H_M) using the conceptual framework developed here.

Acknowledgment. We are very grateful to W. Lubitz and M. Kuhn (Technical University Berlin) and to J. P. Allen and J. C. Williams who generously provided the heterodimer/hydrogen bond *Rhodobacter sphaeroides* strains used in this work. This work was funded in part by a grant from the NSF Biophysics Program.

References and Notes

(1) Deisenhofer, J.; Michel, H. *Science* **1989**, *245*, 1463−1473.
(2) Kirmaier, C.; Holten, D. In *Photosynthesis Research*; Martinus Nijhoff Publishers: Dordrecht, 1987; Vol. 13, pp 225−260.
(3) Boxer, S. G. In *Annual Review of Biophysics and Biophysical Chemistry*; Engelman, D. M., Ed.; Annual Reviews, Inc.: Palo Alto, CA, 1990; Vol. 19, pp 267−99.
(4) Hammes, S. L.; Mazzola, L.; Boxer, S. G.; Gaul, D. F.; Schenck, C. C. *Proc. Natl. Acad. Sci. U.S.A.* **1990**, *87*, 5682−5686.
(5) Lockhart, D. J.; Boxer, S. G. *Proc. Natl. Acad. Sci. U.S.A.* **1988**, *85*, 107.
(6) Parson, W. W.; Warshel, A. *J. Am. Chem. Soc.* **1987**, *109*, 6152.
(7) Lathrop, E. J. P.; Friesner, R. A. *J. Phys. Chem.* **1994**, *98*, 3050−3055.
(8) Lathrop, E. J. P.; Friesner, R. A. *J. Phys. Chem.* **1994**, *98*, 3056−3066.
(9) (9)Middendorf, T. R.; Mazzola, L. T.; Lao, K.; Steffen, M. A.; Boxer, S. G. *Biochim. Biophys. Acta.* **1993**, *1143*, 223.
(10) Stocker, J. W.; Taguchi, A. K. W.; Murchison, H. A.; Woodbury, N. W.; Boxer, S. G. *Biochemistry* **1992**, *31*, 10356−10362.
(11) Lin, X.; Murchison, H. A.; Nagarajan, V.; Parson, W. W.; Williams, J. C.; Allen, J. P. *Proc. Natl. Acad. Sci. U.S.A.* **1994**, *91*, 10265−10269.
(12) Allen, J. P.; Artz, K.; Lin, X.; Williams, J. C.; Ivancich, A.; Albouy, D.; Mattioli, T. A.; Fetsch, A.; Kuhn, M.; Lubitz, W. *Biochemistry* **1996**, *35*, 6612−6619.
(13) Bylina, E. J.; Youvan, D. C. *Proc. Natl. Acad. Sci. U.S.A.* **1988**, *85*, 7226−7230.
(14) Kirmaier, C.; Holten, D.; Bylina, E. J.; Youvan, D. C. *Proc. Natl. Acad. Sci. U.S.A.* **1988**, *85*, 7562−7566.
(15) Fajer, J.; Brune, D. C.; Davis, M. S.; Forman, A.; Spaulding, L. D. *Proc. Natl. Acad. Sci. U.S.A.* **1975**, *72*, 4956−4960.
(16) Boxer, S. G.; Middendorf, T. R.; Lockhart, D. J. *FEBS Lett.* **1986**, *200*, 237.
(17) Middendorf, T. R.; Mazzola, L. T.; Gaul, D. F.; Schenck, C. C.; Boxer, S. G. *J. Phys. Chem.* **1991**, *95*, 10142.
(18) Lyle, P. A.; Kolaczkowski, S. V.; Small, G. J. *J. Phys. Chem.* **1993**, *97*, 6924−6933.
(19) Friesner, R. A.; Won, Y. *Biochim. Biophys. Acta* **1989**, *977*, 99−122.
(20) Middendorf, T. R.; Mazzola, L. T.; Boxer, S. G., unpublished results.
(21) King, B. A.; Stanley, R.; Boxer, S. G., submitted for publication.
(22) Rice, O. K. *J. Chem. Phys.* **1933**, *1*, 375.
(23) Fano, U. *Phys. Rev.* **1961**, *124*, 1866.
(24) Sturge, M. D.; Guggenheim, H. J.; Pryce, M. H. L. *Phys. Rev. B* **1970**, *2*, 2459.
(25) Marcus, R. A.; Sutin, N. *Biochim. Biophys. Acta* **1985**, *811*, 265−322.
(26) Jortner, J. *J. Chem. Phys.* **1975**, *64*, 4860.
(27) Hopfield, J. J. *Proc. Natl. Acad. Sci. U.S.A.* **1974**, *71*, 3640.
(28) Huang, K.; Rhys, A. *Proc. R. Soc. London* **1950**, *A204*, 406.
(29) Markham, J. J. *Rev. Mod. Phys.* **1959**, *31*, 956.
(30) Hush, N. *Prog. Inorg. Chem.* **1967**, *8*, 391.
(31) Zhou, H.; Boxer, S. G., to be published.
(32) Creutz, C.; Taube, H. *J. Am. Chem. Soc.* **1969**, *91*, 3998.
(33) Schenck, C. C.; Blankenship, R. E.; Parson, W. W. *Biochim. Biophys. Acta* **1982**, *680*, 44−49.
(34) Simpson, W. T.; Peterson, D. L. *J. Chem. Phys.* **1957**, *26*, 588.
(35) Moore, L. J.; Zhou, H.; Boxer, S.G., to be published.
(36) Schenck, C. C.; Gaul, D.; Steffen, M.; Boxer, S. G.; McDowell, L.; Kirmaier, C.; Holten, D. In *Reaction Centers of Photosynthetic Bacteria*; Michel-Beyerle, M. E., Ed.; Springer-Verlag: Berlin Heidelberg, 1990; Vol. 6; pp 229−238.
(37) Williams, J. C.; Alden, R. G.; Murchison, H. A.; Peloqiun, J. M.; Woodbury, N. W.; Allen, J. P. *Biochemistry* **1992**, *31*, 11029−37.